JOURNAL OF GEOPHYSICAL RESEARCH, VOL. 103, NO. D5, PAGES 5747–5758, MARCH 20, 1998

Trifluoroacetic acid from degradation of HCFCs and HFCs: A three-dimensional modeling study

V. R. Kotamarthi, J. M. Rodriguez, M. K. W. Ko, T. K. Tromp, and N. D. Sze
Atmospheric and Environmental Research, Inc., Cambridge, Massachusetts

Michael J. Prather
Earth System Science, University of California, Irvine

Abstract. Trifluoroacetic acid (TFA; CF_3COOH) is produced by the degradation of the halocarbon replacements HFC-134a, HCFC-124, and HCFC-123. The formation of TFA occurs by HFC/HCFC reacting with OH to yield CF_3COX (X = F or Cl), followed by in-cloud hydrolysis of CF_3COX to form TFA. The TFA formed in the clouds may be reevaporated but is finally deposited onto the surface by washout or dry deposition. Concern has been expressed about the possible long-term accumulation of TFA in certain aquatic environments, pointing to the need to obtain information on the concentrations of TFA in rainwater over scales ranging from local to continental. Based on projected concentrations for HFC-134a, HCFC-124, and HCFC-123 of 80, 10, and 1 pptv in the year 2010, mass conservation arguments imply an annually averaged global concentration of 0.16 μg/L if washout were the only removal mechanism for TFA. We present 3-D simulations of the HFC/HCFC precursors of TFA that include the rates of formation and deposition of TFA based on assumed future emissions. An established (GISS/Harvard/UCI) but coarse-resolution (8° latitude by 10° longitude) chemical transport model was used. The annually averaged rainwater concentration of 0.12 μg/L (global) was calculated for the year 2010, when both washout and dry deposition are included as the loss mechanism for TFA from the atmosphere. For some large regions in midnorthern latitudes, values are larger, 0.15–0.20 μg/L. The highest monthly averaged rainwater concentrations of TFA for northern midlatitudes were calculated for the month of July, corresponding to 0.3–0.45 μg/L in parts of North America and Europe. Recent laboratory experiments have suggested that a substantial amount of vibrationally excited CF_3CHFO is produced in the degradation of HFC-134a, decreasing the yield of TFA from this compound by 60%. This decrease would reduce the calculated amounts of TFA in rainwater in the year 2010 by 26%, for the same projected concentrations of precursors.

1. Introduction

The long-lived fully halogenated organic compounds are being replaced by hydrofluorochlorocarbons (HCFCs) and hydrofluorocarbons (HFCs). Because of removal by reaction with OH in the troposphere, smaller tropospheric accumulations for these chemicals are expected [*World Meteorological Organization* (*WMO*), 1990; *Intergovernmental Panel on Climate Change* (IPCC), 1990; *Rodriguez et al.*, 1993; *Kanakidou et al.*, 1995], leading to smaller global ozone depletion potentials and global warming indices. Another criterion for the acceptability of the substitute HCFCs/HFCs pertains to the impact of these compounds or their degradation products on ecosystems.

Trifluoroacetic (TFA; CF_3COOH) is produced from the atmospheric degradation of HFC-134a (CF_3CH_2F), HCFC-124 (CF_3CHFCl), and HCFC-123 (CF_3CHCl_2). It is highly soluble in water and expected to be removed from the atmosphere mainly by washout. Globally averaged concentrations of TFA in rainwater (μg/L) r_{TFA} can be easily estimated from mass-balance considerations. Adopting molar yields for TFA of 33% yield from HFC-134a (see discussion in section 5.6 for impact of other possible yields) and 100% for HCFC-123 and 124, a global rainfall rate of 5×10^{17} L/yr [*Jaeger*, 1983] and an emission scenario for the HCFC/HFCs provided by D. Hufford (1993), the global average r_{TFA} concentrations for the year 2010 is about 0.16 μg/L, assuming that washout is the dominant loss mechanism for gas phase TFA.

Local r_{TFA} values deviate from the global averages due to inhomogeneities in OH concentrations and precipitation rates, as well as the long-range transport of gas phase. TFA and its precursors. Evaluation of the impact of these processes requires models ranging in scales from global to regional. The global distribution of TFA in rainwater produced from HFC-134a alone has been previously studied with a two-dimensional (2-D) model [*Rodriguez et al.*, 1993]. *Kanakidou et al.* [1995] modeled the fate of a series of CFC replacements, including TFA precursors, with a 3-D model using monthly average wind fields and full chemistry.

In this paper we present the global distribution of TFA in the gas phase and in precipitation produced by the degradation of HFC-134a, HCFC-124, and HCFC-123 using a coarse grid chemical transport model (CTM), but including synoptic scale weather patterns, diurnal boundary layers, and wet and dry convective plume mixing processes derived from a general circulation model (GCM). Observed climatological values of

Paper number 97JD02988.
0148-0227/98/97JD-02988$09.00

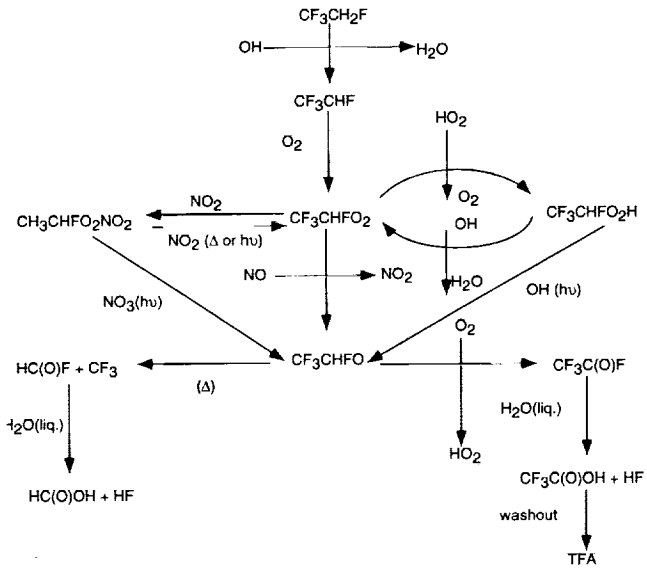

Figure 1. Degradation pathway for HFC-134a from *Franklin* [1993]. Diagram shows mechanisms that lead to the formation of TFA. CF_3 radical formed in the end undergoes several other reactions, which are of no importance to the topic discussed here.

cloud cover and rainfall were used to calculate hydrolysis and washout rates. On an annual average basis in midnorthern latitudes, r_{TFA} concentrations are 0.15–0.20 μg/L in specific grid boxes, but for particular months they are as large as 0.3–0.45 μg/L. Modeling uncertainties due to assumed liquid water and precipitation patterns are also presented.

No deleterious effects have been identified for the expected water concentrations of less than 0.5 μg/L. Concerns have been raised about the long-term accumulation of trifluoroacetic acid in certain aquatic environments. Since TFA seems to be remarkably stable in the biosphere/hydrosphere, *Tromp et al.* [1995] suggested that accumulation of TFA in certain closed aquatic systems over several decades could increase TFA concentrations to factors of 100 times rainwater concentrations. The study presented in this paper provides values for rainwater concentrations averaged over areas of the order of 800 × 1000 km. This information can be used to assess the effect of long-term accumulation by obtaining more information on the local hydrological conditions, atmospheric degradation of TFA precursors, and the local deposition fluxes and the local concentrations in rainwater of TFA. Individual aquatic environments in a suspected impact area must be studied by using hydrological models with the drainage basin characteristics of the area.

The degradation pathways for the precursor HFC and HCFCs are discussed in section 2. A brief description of the chemical model, input data sets used for rainfall and cloud cover, and approximations used for calculating cloud and precipitation processes are presented in section 3. Section 4 presents the results of the simulations. Sensitivity calculations for noted uncertainties are discussed in section 5. Conclusions and recommendations for further research are found in section 6.

2. Degradation Pathway for HFC/HCFCs

Our simulation of TFA concentrations in rainwater requires calculation of the net yield of TFA in the degradation of HCFC/HFCs, which has been the subject of intense research for the past decade. Schemes originally proposed in analogy with those of fully saturated hydrocarbons [*WMO*, 1990] were proven correct by numerous kinetic measurements [e.g., *NASA*, 1994]. We review here the degradation of the three TFA precursors, HFC-134a, HCFC-123, and HCFC-124, whose main atmospheric sink is initiated by reaction with OH in the troposphere. Stratospheric removal occurs also through photolysis and less so by reaction with $O(^1D)$.

Figure 1 shows our current understanding of the degradation pathways for HFC-134a [*Franklin*, 1993]. Analogous degradation mechanisms have been described for HCFC-123 and 124 [see *WMO*, 1990]. Consideration of the degradation pathways in Figure 1 indicates that the TFA rainout is a major pathway for final removal of the trifluoroacetyl fluoride, $CF_3C(O)F$, from the troposphere. The actual yield of TFA will depend on the competing photochemical pathways for the degradation of alkoxy radical (CH_3CHFO). One option is that the complete photochemical scheme be included in a 3-D CTM; however, transport will affect the geographical distribution of TFA only through its impact on those intermediate products whose lifetimes are longer than a few days in the lower troposphere, where most of the rainout occurs. Thus we simplified the chemical scheme and were able to carry out a larger number of sensitivity studies.

For the purposes of the TFA simulations the schemes for precursor degradation (Figure 1) were simplified to those shown in Figure 2, in which only three species with lifetimes longer than a few days in the lower troposphere are carried in the CTM as prognostic variables. These include the precursor

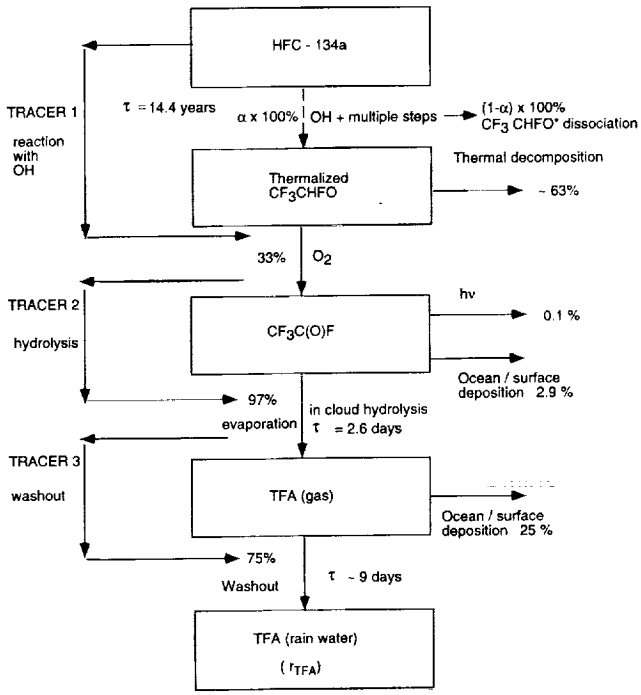

Figure 2a. Degradation pathways for HFC-134a. The reaction pathway is highly simplified and does not show many short-lived intermediate compounds. The three step TFA formation mechanism hypothesized for the 3-D simulation is shown on the left of the figure. Percentages denote the calculated molar fraction on each box degraded through the indicated channel. See text for discussion of α.

HCFC/HFC, an intermediate trifluoroacetyl halide of the form $CF_3C(O)X$ (X = F, Cl), and gas phase TFA. Figures 2a, 2b, and 2c show the intermediate steps in the formation of TFA from HFC-134a, HCFC-123, and HCFC-124. Local photochemical steady state is assumed for all the other species not explicitly included in this scheme.

2.1. Removal of Precursor HCFC/HFC and Production of $CF_3C(O)X$

As indicated, in Figure 2, the removal of the precursors occurs through reaction with tropospheric OH. The reaction of HFC/HCFC with OH leads to production of CF_3CXYO through multiple and rapid intermediate steps (where X = F, Y = H for HFC-134a; X = Y = Cl for HCFC-123; and X = F, Y = Cl for HCFC-124).

$$P(CF_3CXYO, r, t) = k_{OH}(T)[OH](r, t)[HCFC/HFC](r, t) \quad (1)$$

where $P(CF_3CXYO, r, t)$ ($cm^{-3}\ s^{-1}$) denotes the production of CF_3CXYO at each location r and time t; $k_{OH}(T)$ ($cm^3\ s^{-1}$) is the reaction rate (a function of local temperature (T)) of the corresponding HCFC/HFC with OH; and the local concentrations (cm^{-3}) of OH and HCFC/HFC are denoted by brackets. The rate constants (k_{OH}) adopted for the reaction of HFC-134a, HCFC-123, and HCFC-124 with OH are from *DeMore et al.* [1992].

Particular attention must be paid to the degradation of HFC-134a. The radical CF_3CFHO is produced in the atmosphere mainly via reaction of CF_3CHFO_2 with NO. Laboratory data reported by *Wallington et al.* [1996] indicate that the CF_3CHFO is produced initially in an excited state

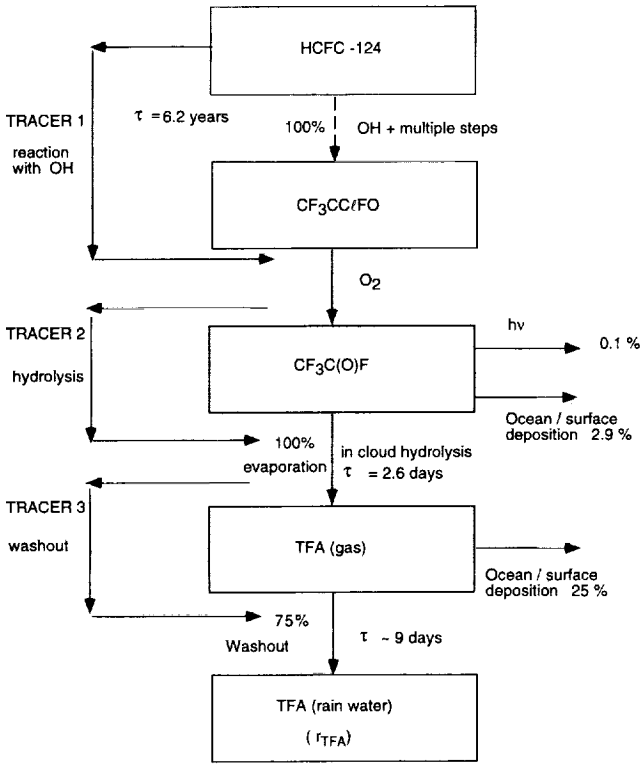

Figure 2b. Same as 2a but for HCFC-124. We assume that all CF_3CClFO is thermalized.

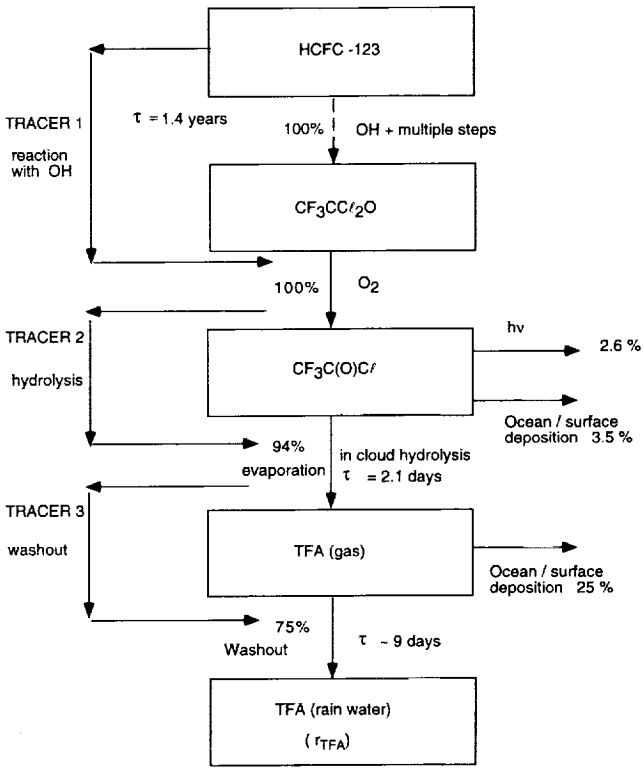

Figure 2c. Same as 2a but for HCFC-123. We assume that all CF_3CCl_2) is thermalized.

(CF_3CHFO^*). A fraction 1-α undergoes rapid dissociation through C-C fission, while the remaining fraction α becomes deexcited by thermal collisions. The thermalized alkoxy intermediate CF_3CFHO can either form CF_3COF after losing the H atom through reaction with O_2 or undergo thermal fission of the carbon-carbon bond.

$$CF_3CFHO + O_2 \rightarrow CF_3COF + HO_2\ (k_2;\ cm^3\ s^{-1}) \quad (2)$$

$$CF_3CFHO \rightarrow CF_3 + HCOF\ (k_3;\ s^{-1}). \quad (3)$$

Taking into account the possibility of prompt dissociation of CF3CHFO* in the atmosphere, the molar yield of CF_3COF from degradation of HFC-134a is given by

$$y_{134a} = \alpha \frac{k_2(T)[O_2]}{k_3(T) + k_2(T)[O_2]} = \alpha \frac{[O_2]}{K(T) + [O_2}} \quad (4)$$

where $K(T)$ (cm^{-3}) = $(k_3(T)/k_2)$). The rates k_2 and k_3 have been measured by *Tuazon and Atkinson* [1993] and *Wallington et al.* [1992]. The reported values of *Wallington et al.* [1992] agree with those of *Tuazon and Atkinson* [1993] when the rate expression for K of *Wallington et al.* [1992] is expressed in a pressure dependent format as shown in Table 1. *Wallington et al.* [1996] reported a value of 0.4 for α. We note, however, that the calculations presented below assume a value of α = 1.0. The impact of the recent value of Wallington et al. is discussed in section 5.6.

By contrast, the alkoxy radicals CF_3Cl_2O and CF_3ClFO, produced in the degradation of HCFC-124 (Figure 2b) and HCFC-123 (Figure 2c), respectively, undergo chlorine abstraction leading to the formation of CF_3COX [*Atkinson*, 1989], with

Table 1. List of Reaction Rate and Hydrolysis Rate Constants Used in the Model

Species	Constant	Reference
CF_3COF	H = 3.2 (M/atm) (Henry's law constant)	*George et al.* [1993]
CF_3COF	k_h = 147 (1/s) (hydrolysis constant)	*George et al.* [1993]
CF_3COCl	H = 2.5 (M/atm) (Henry's law constant)	*George et al.* [1993]
CF_3COCl	k_h = 200 (1/s) (hydrolysis constant)	*George et al.* [1993]
CF3COF	$K(T, M) = \frac{K_0(T)M}{1 + K_0(T)M/K_\infty(T)} F_c^{\{1+[\log_{10}(K_0(T)M/K_\infty(T))]^2\}^{-1}}$	
	where $K_\infty(T) = \frac{1}{1.58 \times 10^{-25}} \exp^{3600/T}$	
	$K_0(T) = \frac{7.35}{3.28 \times 10^{19} * 1.58 \times 10^{-25}} \exp(3600/T)$	
	M = air density molecules/cm^3 F_c = 0.6	

$$y_{123} = y_{124} = 1 \quad (5)$$

We can then express the production of $CF_3C(O)X$ at each model grid point using local steady state

$$P(CF_3C(O)X, r, t)$$

$$= y_{HCFC/HFC}(r, t) k_{OH}(r, t)[OH]((r), t)\,[HCFC/HFC](r, t) \quad (6)$$

where HCFC/HFC denotes HFC-134a or HCFC-124 if X = F, and HCFC-123 if X = Cl. The yields for HCFC-123 and HCFC-124 is 1 and that for HFC-134a is given in (4).

2.2. Degradation of $CF_3C(O)X$

Hydrolysis of $CF_3C(O)X$ in cloud water results in the formation of TFA and is the main loss process for $CF_3C(O)X$. Because of the large grid size (approximately 800 km × 1000 km) in the CTM, the cloud occurrence and hydrolysis are necessarily subgrid-scale processes. The rate-limiting step for the hydrolysis rate is determined by the slowest of several processes, including (1) residence time of air masses inside a cloud, (2) diffusion of the gas molecule to the liquid droplet, (3) diffusion of the molecule into the liquid, and (4) hydrolysis inside the droplet. The analysis of *Schwartz* [1986] shows that the timescales of interest are the hydrolysis time inside the droplets and the residence time of an air parcel inside the clouds.

To address this issue, we adopted the following procedure: *Lelieveld et al.* [1989] have calculated the residence time of an air parcel inside a cloud for different cloud types. The residence time is defined as the ratio of the depth of the cloud and the vertical velocity of air through the cloud for majority of the cloud types. The results indicate the residence times range between 0.2 and 3 hours for various cloud types. Using this definition of residence time, we can approximate the amount of air processed by a cloud in a given grid box during a given time period Δt as the sum of (1) the fraction of initial amount of air within the cloud processed during this time and (2) the fraction of additional volume of air which flows through the cloud in the time period Δt. If the hydrolysis rate is sufficiently fast, we can neglect the fact that different air masses will reside for different lengths of time within the cloud and obtain the following approximate expression for the amount of $CF_3C(O)X$ removed in time step Δt:

$$\Delta[CF_3C(O)X](r, t) = -[CF_3C(O)X](r, t)\, f(r, t) \cdot (1 - \exp(-K_d(r, t)\Delta t))(\Delta t/\tau) \quad (7)$$

where Δt is the hydrolysis time step used in the model, $f(r, t)$ is the fractional cloud volume in the grid, and K_d is discussed below. A hydrolysis time step of 2 hours was used. We adopted a value of 122 hours for τ as an approximate average of the residence times for cumulus and stratus. This τ was used for the entire model domain, and no differentiation was made between upper level, midlevel, and low clouds with respect to the residence times. The sensitivity of the calculations to this assumed residence time is evaluated in section 5.3. We find this formulation to be adequate for the purpose of the present calculations and on the basis of our sensitivity tests on the timescales of hydrolysis involved.

The in-cloud hydrolysis first-order rate K_d (s^{-1}) in (7) is calculated as follows: in the absence of mass transfer constraints the fraction of gas phase $CF_3C(O)X$ that reacts per unit time by dissolving and hydrolyzing in the cloud water is given by [*Kanakidou et al.*, 1993; *Freiberg and Schwartz*, 1980].

$$K_d = f k_h HRT\,(LWC) \quad (8)$$

where H is the Henry's constant (M/atm; M is moles dissolved/liter of solution); LWC is the dimensionless liquid water content of clouds (grams of water/grams of air); R is the gas constant; T is temperature (in °K) and k_h is the hydrolysis constant in rainwater (s^{-1}). Solubility and hydrolysis rate constants for CF_3COF and CF_3COCl are given in Table 1. The factor f denotes a correction factor to compensate for diffusional resistance inside the droplets, corresponding to values of 0.5 for CF_3COCl and 0.65 for CF_3COF [*Kanakidou et al.*, 1995]. The hydrolysis rates calculated by (8) are of the order of 1/min in the presence of clouds. Thus the exponential term in (7) tends to zero for the hydrolysis time step considered here (2 hours), and the amount of CF3C(O)X becomes directly proportional to the cloud cover fraction.

Cloud fraction and liquid water content of the clouds were estimated from the zonally averaged data described by *Lelieveld et al.* [1989]. This data set contains cloud cover and liquid water content of the clouds on a 10° latitude by 100 mbar resolution and has been used by *Lelieveld and Crutzen* [1990] to study the effect of liquid phase chemistry on ozone levels in the troposphere. The data set used has averaged information for the four seasons. The zonally averaged data were mapped on to a three-dimensional grid using the climatological monthly averaged surface rain data of *Shea* [1986] as a weighting factor. Figure 3 shows the annual average and column-integrated liquid water. Large-scale features of the liquid water distribution are qualitatively consistent with observations [*Prabhakara et*

al., 1983], but a detailed comparison with other data sets, such as ISCCP (International Cloud Climatology Project), is beyond the scope of this work.

We also assumed that the cloud fraction given for a grid box is constant throughout the month. Thus there is no cloud free period for the entire grid box if the data suggest the existence of clouds at the beginning of each month. The usage of surface rainfall statistics to map the 2-D fractional cloud coverage and liquid water content data onto the 3-D grid seems reasonable, since excluding a few locations, persistent cloudiness is indicative of high monthly average precipitation [*Wallace and Hobbs*, 1977]. There are a few exceptions, where persistent nonprecipitating low-level cloud decks are observed, with little or no accompanying rainfall. The sensitivity of calculated r_{TFA} to our assumption of cloud frequency is discussed in section 5.1.

We also included photolysis and dry deposition of $CF_3C(O)X$ in the simulations. CF_3COF is photolyzed slowly in the troposphere and has photolysis lifetimes of the order of thousands of years [*Rattigan et al.*, 1991]. CF_3COCl produced from HCFC-123 (Figure 2c) is photolyzed at a much faster rate in the troposphere with photolysis lifetimes of the order of weeks [*Wallington et al.*, 1994]. These photolysis channels do not lead to production of TFA. We adopted a dry deposition velocity of 0.3 cm/s for $CF_3C(O)X$ over both land and ocean surfaces.

2.4. Production of Gas Phase TFA in the Atmosphere

Hydrolysis of CF_3COX in cloud water produces $CF_3C(O)OH$ (TFA). TFA is a strong acid with a pK of 0.25 [*Exner et al.*, 1992] and is expected to dissociate immediately and form $CF_3C(O)O^-$. Upon cloud reevaporation this anion will probably reevaporate as gas phase $CF_3C(O)OH$ or remain a CF_3COO^- in residual aerosol. In either case we assume that both forms will again dissociate after reincorporation into cloud or rainwater. TFA was assumed to undergo full evaporation as many times as the cloud water itself within each grid box and time step. In this case, the production of gas phase TFA in the model time interval Δt is given by

$$P(\mathrm{TFA}, r, t) = -\Delta[CF_3C(O)X](r, t)/\Delta t \qquad (9)$$

where $\Delta[CF_3C(O)X]$ is discussed in the previous section. If CF_3COO^- is incorporated into stable salts which do not further dissociate, the production of gas phase TFA would be much smaller than calculated below.

2.5. Removal of Gas Phase TFA

TFA is highly soluble (Henry's constant of $> 10^7\ M\ \mathrm{atm}^{-1}$ [*Wine and Chameides*, 1990]) and hence can be expected to be rained-out at a rate similar to that of HNO_3, which has a global average washout rate of about 9 days. We parameterized TFA washout as a continuous process, using the altitude dependent, globally averaged first-order loss rates of nitric acid [*Logan et al.*, 1981]. To account for spatial variations, the specified washout rates were mapped onto a three-dimensional grid using the climatological surface precipitation data of *Shea* [1986] as a weighting factor. This approach is new with this CTM; we neglect the coupling between rainout and convective and/or large-scale precipitation (see discussion by *Balkanski et al.* [1993]).

Dry deposition of TFA was modeled by assuming a constant deposition velocity of 2 cm/s overland and 0.3 cm/s over ocean surfaces at rates approximately similar to those used for HNO_3 [*Kotamarthi and Carmichael*, 1990]. The deposition velocities over the ocean surface are lower as the surface roughness over the ocean is smaller, increasing the transfer resistance of the gas phase TFA to the ocean surface. Rates for the reactions of gas phase $CF_3C(O)OH$ with OH have been measured [*Carr et al.*, 1994]. *Kanakidou et al.* [1995] estimated that inclusion of this process would decrease the calculated TFA in rainwater (r_{TFA}) by at most 5% and much less if a large fraction of the reevaporated anion takes the form of a salt. We have not included this process in our calculations.

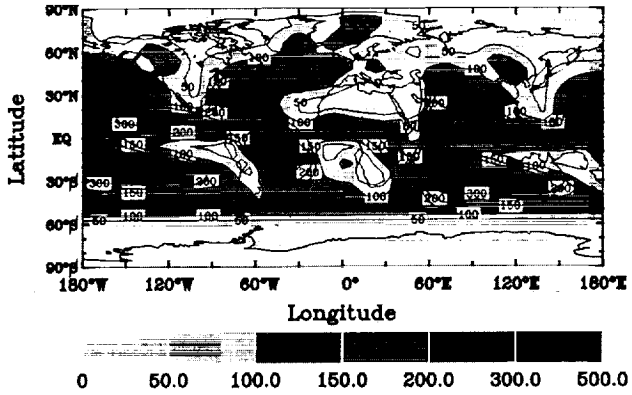

Figure 3. Annual average column-integrated cloud liquid water content (gm/m^2).

3. Description of Model and Input Data

The 3-D CTM developed at GISS (Goddard Institute for Space Science)/Harvard/UCI (University of California at Irvine) was used for simulating the 3-D distribution of the trace species of interest. This model uses a 1 year output of wind data and convection statistics (every 4 hours) from the GISS GCM [*Hansen et al.*, 1983]. This data set is recycled for multiple-year runs. The interhemispheric transport in this model has been previously tested through comparisons with measurements of long-lived fluorocarbons, CH_3CCl_3 and ^{85}Kr [*Prather et al.*, 1987; *Jacob et al.*, 1987]. The model reproduced observations satisfactorily after corrections were applied to the transport scheme to include a horizontal diffusion term to improve the north-south hemispheric exchange [*Prather et al.*, 1987]. Vertical transport by convection was tested through comparisons to ^{222}Rn [*Jacob and Prather*, 1990]. A coarse-grid tropospheric version of the model, with a horizontal resolution of 8° latitude by 10° longitude and nine grid points in the vertical extending from the surface of 10 mbar was used in the present study. There are seven grid points in the troposphere and in the stratosphere.

Simulations of the concentrations of TFA in rainwater were carried out by simultaneous calculations of three sets of tracers (see Figure 2): (1) the precursor HCFC/HFC, (2) the long-lived halocarbonyls of the form $CF_3C(O)X$, and (3) gas/particle phase TFA. Production and loss of these tracers are incorporated in the model as described in section 2. The parameterizations for these processes require input of (1) emission scenarios and geographical distribution for precursors HCFC/HFCs, (2) global fields of OH for destruction of precursors in troposphere, and (3) three-dimensional distributions

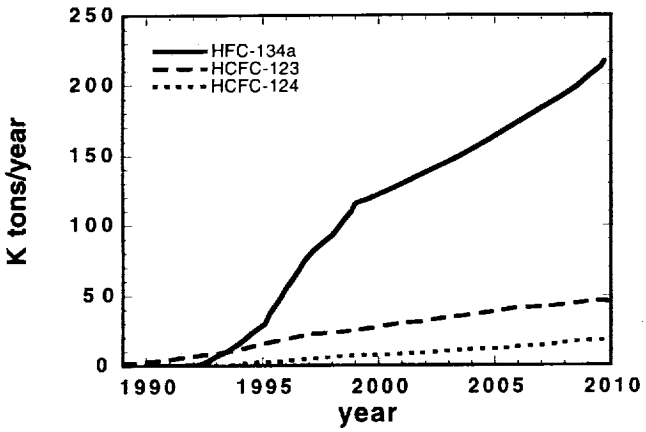

Figure 4. Emission scenario for the three TFA precursors used in the study [*Hufford*, 1993].

of liquid water content and precipitation to estimate rates of hydrolysis and washout.

The emissions of precursors between 1985 and 2010 were prescribed according to the scenario shown in Figure 4, which predicts HFC-134a to be in wider use than HCFC-124 or HCFC-123 during the next decade (D. Hufford, 1993). Other emission scenarios suggest that the emissions in Figure 4 could easily change by factors of 2 [*Kanakidou et al.*, 1995]. The emissions were distributed around the globe using the electric power consumption statistics as a weighting factor following *Prather et al.* [1987]. This emission distribution is similar to the chlorofluorocarbon emission inventory of *McCulloch et al.* [1994].

A global scale OH field derived for this model, using a parameterized chemistry scheme by *Spivakovsky et al.* [1990], was used to calculate the loss of HFC-134a, HCFC-124, and HCFC-123 by reaction with OH. The above authors calculated this field based on available and assumed global distributions of H_2O, CO, CH_4, NO_x, and O_3. The CH_3CCl_3 lifetime calculated by using the model is 5.8 years. This lifetime indicates that the global OH calculated in this model is about 20% lower than the latest recommendations [*Prinn et al.*, 1995; *IPCC*, 1996]. The sensitivity of the calculated r_{TFA} to a 20% change in the OH fields is discussed in section 5.5.

A precipitation climatology based on a historical set of observations from the year 1950 to 1979 [*Shea*, 1986] was used in this study to scale the washout rates, cloud cover fractions, and liquid water content of the clouds. Data are available to produce the total rainfall contours for each month on a 2.5 latitude by 2.5 longitude grid. Full longitudinal coverage is derived from 45°S to 90 °N. For completeness we appended the zonal mean rainfall data from the *Jaeger* [1976] climatology to the Shea data south of 45°S in order to include the effect of removal in this region. However, because of uncertainties in the rainfall climatology we ignore results south of 60°S and north of 80°N. The sensitivity of the calculated midlatitude r_{TFA} to the uncertainties in the rainfall amounts from 60°S to 90°S is discussed in section 5.

Time dependent calculations were carried out between the years 1989 and 2010 separately for HCFC-123, HCFC-124, and HFC-134a by varying the surface fluxes of these species according to the emission scenario in Figure 3. The model was initialized in 1985 with negligible mixing ratios of the precursors and degradation products $CF_3C(O)X$ and TFA. All other production and loss processes were kept constant throughout the simulation, since predicted changes in overhead ozone and tropospheric OH are not expected to change our results substantially, and we cannot reliably predict the secondary chemical effects.

4. Results

4.1. Concentrations and Distribution of Precursors

The calculated global average mixing ratios for HFC-134a, HCFC-124, and HCFC-123 between 1985 and 2010 are shown in Figure 5. We obtain values of 80 pptv for HFC-134a, 9.8 pptv for HCFC-124, and 1.1 pptv for HCFC-123 in 2010. Model-calculated lifetimes for HFC-134a, HCFC-124, and HCFC-123 are 14.4, 6.2, and 1.4 years, respectively. These are within the uncertainties of the latest recommendations for these species [*IPCC*, 1996; *Prather and Spivakovsky*, 1990].

The calculated surface distributions of HFC-134a for the year 2010 are shown for the month of July in Figure 6. The largest gradients are calculated near the equator and close to major sources. The southern hemisphere mixing ratios average 78 ppt during July (southern hemisphere winter) and the northern hemisphere mixing ratios average about 90 ppt. The January mixing ratios in the southern hemisphere (not shown here) are almost uniform at about 73 ppt and above 85 ppt in the northern hemisphere.

Figure 7 shows the calculated surface distribution of HCFC-

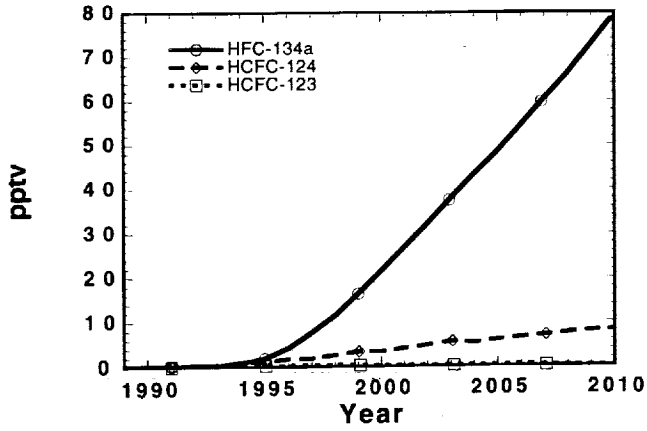

Figure 5. Global average mixing ratios (pptv) for HFC-134a, HCFC-124, and HCFC-123.

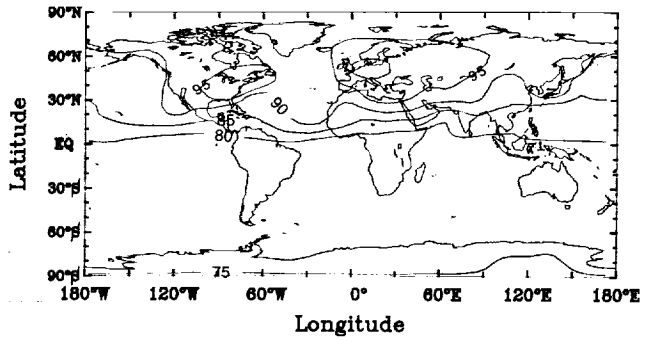

Figure 6. HFC-134a surface distribution for the month of July in the year 2010 in units of pptv. Contour levels at 75, 80, 85, 90, 95, and 110 pptv.

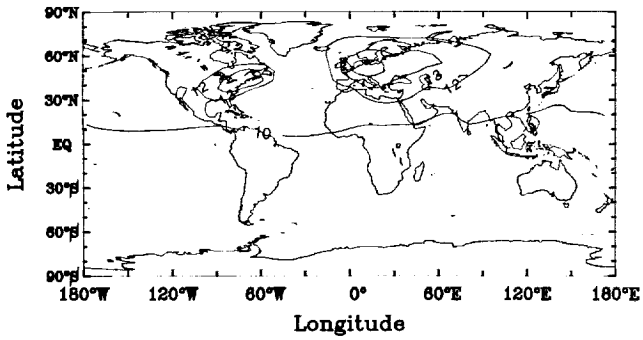

Figure 7. HCFC-124 surface distribution for the month of July in the year 2010 in units of pptv. Contour levels at 8, 10, 12, 13, and 15 pptv.

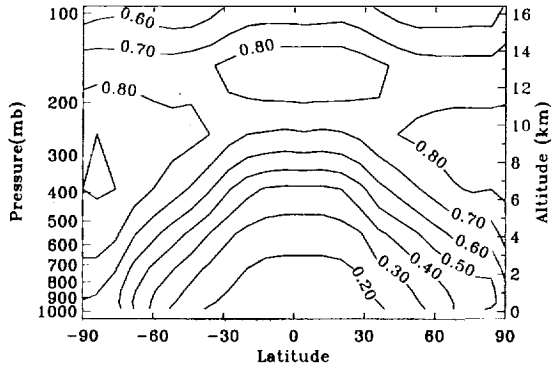

Figure 9. Zonal average mass yield of CF_3COF from HFC-134a calculated by using the kinetic data of *Wallington et al.* [1992] and a value of $\alpha = 1$ in equation (4).

124 for the year 2010 for the month of July. The southern hemisphere mixing ratios are between 10 and 8 pptv for the winter months. Figure 8 shows the calculated surface distribution of HCFC-123 for the year 2010 for the months of July. HCFC-123 has a much shorter lifetime of 1.4 years, producing the largest gradients. The southern hemisphere mixing ratios are less than 1 ppt for July.

4.2. Distribution and Fate of $CF_3C(O)X$

Kinetic data [*Wallington et al.*, 1992; *Tuazon and Atkinson*, 1993] indicate that the yields of CF_3COF from HCFC-124 and CF_3COCl from HCFC-123 are close to 100% on mole basis, corresponding to 87 and 85% on a mass basis for 123 and 124, respectively. Figure 9 shows the calculated mass yields of CF_3COF from HFC-134a as a function of latitude and height. Each latitude points represents an average value for all the longitudes in that latitude/altitude level. Small yields of (~0.2) near the surface increase to larger yields (~0.8) in the upper troposphere. The calculated global-average mass yield of CF_3COF from HFC-134a was 0.37.

The mass percentages of $CF_3C(O)X$ lost by the different processes are summarized in Table 2. Cloud hydrolysis, the channel producing TFA, by far dominates all the $CF_3C(O)X$ degradation mechanisms. Tropospheric lifetimes of 2.6 and 2.1 days are calculated for $CF_3C(O)F$ and $CF_3C(O)Cl$, respectively.

Figures 10a and 10b show the surface distribution of CF_3COF and the zonal average latitude-height distribution of CF_3COF, respectively, for the month of July for the year 2010.

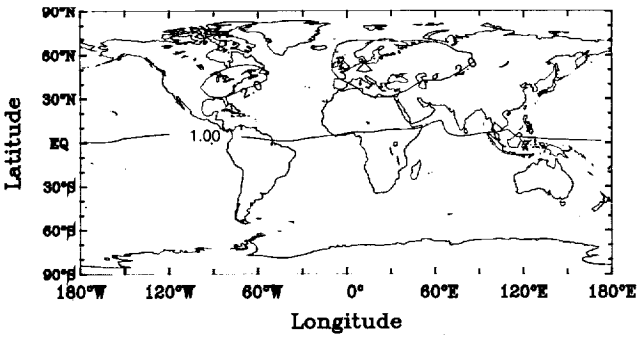

Figure 8. HCFC-123 surface distribution for the month of July in the year 2010 in units of pptv. Contour levels at 0.65, 1.0, 2.0, 3.5, and 4.0 pptv.

The surface distribution of CF_3COF (Figure 10a) shows higher mixing ratios in the tropical regions and near-source locations in western Europe and North America. The zonal mean cross section shows increasing mixing ratios with altitude. CF_3COF in the lower and middle troposphere is rapidly removed by hydrolysis in clouds resulting in lower mixing ratios. Figures 11a and 11b show the surface distribution of CF_3COCl and its zonal average latitude-height distribution, respectively, for the month of July for the year 2010. The surface mixing ratio distribution of CF_3COCl (Figure 11a) again shows features similar to those of CF_3COF, with maximum mixing ratios in near-source locations and in the subtropical regions. The zonal-mean cross section shows a similar behavior compared to CF_3COF. The mixing ratios decrease with altitude in the tropical and mid-latitude region up to a height of 700 mbar, corresponding to the maxima in cloud cover fraction climatology adopted by us. At altitudes from 700 mbar to the tropopause levels the mixing ratios increase. At altitudes corresponding to the stratosphere in the model, the mixing ratios decrease again, as the photolytic loss of CF_3COCl starts controlling its distribution.

4.3. Deposition and Rainwater Concentrations of TFA

We consider two parameters which could be of interest in evaluating the effect of TFA on a given environment. These are (1) the deposition fluxes (mass/unit area) of TFA at a given location and (2) the concentration of TFA in rainwater (r_{TFA}). The deposition fluxes could be a useful input for estimates of accumulations of TFA over an extended period of time, particularly if we are interested in evaluating the input to a large stable water reservoir or soil. Concentrations of TFA in rainwater are more pertinent to evaluate the concentrations in "seasonal" water bodies produced each year exclusively by local rainfall and whose content is wholly determined by yearly rainfall and possible year-to-year accumulation [*Tromp et al.*, 1995].

Table 2. Percent of $CF_3C(O)X$ (Global Average by Mass) Lost Through Different Processes Modeled

Process	$CF_3C(O)F$	$CF_3C(O)Cl$
Photolysis	0.1%	2.6%
Surface deposition	2.9%	3.5%
Hydrolysis	97%	93.9%

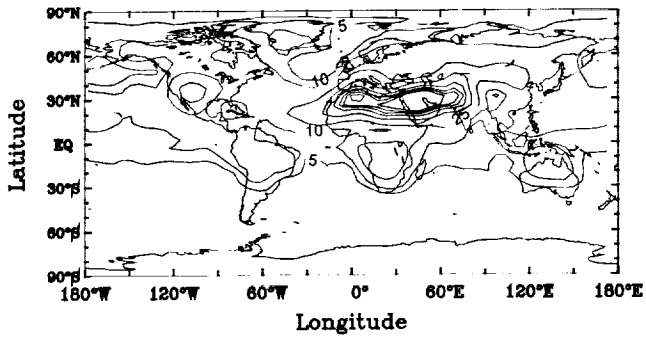

Figure 10a. Surface distribution of CF_3COF (1.0E-3 pptv) for the month of June in the year 2010. Contour are at 5, 10, 25, 50, 75, 90, 100, and 110.

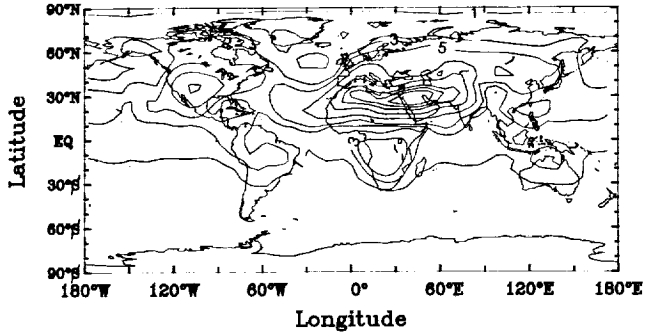

Figure 11a. Surface distribution of CF_3COCl (1.0E-3 pptv) for the month of July in the year 2010. Contours ar at 1, 3, 5, 10, 20, 30, and 40.

Fluxes of TFA deposited by the washout process, accumulated over the period of simulation (1989–2010) in mg/m^2 are shown in Figure 12. Since most of the CF_3COX is formed from HFC/HCFCs in the tropical regions and CF_3COF is converted to TFA with a very short lifetime (local lifetimes of the order of hours), production of TFA maximizes in the tropics. Typical washout time constants in the tropics are 3 days. These time constants are much smaller than typical meridional transport time constants (weeks to months), and most of the TFA produced in the tropical regions is deposited in these regions. Figure 13 shows the cumulative amount of TFA deposited due to both the wet and the dry deposition processes, from 1985 to 2010. Comparison of Figure 13 and 12 indicates that our calculated dry deposition fluxes are of the order of 20% of the wet deposition fluxes.

Figure 14 shows the calculated annual average r_{TFA} concentrations (μg/L) for the year 2010. The rainwater concentration of TFA is defined as the ratio of total TFA deposition by washout over a grid box (liters/month) to the rainfall received in the grid box (liters/month). Thus r_{TFA} concentration may be inversely related to the rainfall received in a particular grid box. The maximum r_{TFA} concentrations are indeed found in the region close to maximum TFA production and receiving the least amount of rainfall. Region in southwestern United States and southern Europe have concentrations of up to 0.2 μg/L. However, as discussed below, the obtained distribution is not simply given by a balance of local production and washout of TFA; transport of precursors and gas phase. TFA also plays an important role. The global average r_{TFA} is 0.12 μg/L, and the subtropical and regions of western Asia have the highest r_{TFA} concentrations of up to 0.3 μg/L. The highest concentrations at any given location in the northern hemisphere were obtained for the month of July 2010: 0.45 μg/L at locations in southern Europe, 0.3 μg/L for most of North America and Europe, and up to 0.4 μg/L for parts of North America and southern Europe.

Because of the fairly long meridional transport time constants, 2-D model calculations have obtained concentrations of TFA in rainwater which can be approximately obtained by local balance between production and loss within a latitude band [*Rodriguez et al.*, 1993]. This is not the case for the zonal asymmetries that show up in this CTM calculation. The annual average ratio of maximum r_{TFA} concentration obtained in a grid box to the global average r_{TFA} concentration of 0.12 μg/L for the year 2010 can be obtained from Figure 14. The maximum asymmetry is of the order of 2.5 and is obtained in western Asia. Concentrations in most of North America and southern Europe are up to a factor of 1.5 higher than the global average. In southern United States the r_{TFA} concentrations are up to a factor 2 higher than the global average concentrations. As a reference, Figure 15 shows the annual average rainfall amounts used in the simulation, scaled by the global mean and then inverted. In the absence of transport we would expect that the asymmetries in r_{TFA} would correlate to those in Figure 15. This is illustrated in Figure 16, which shows the calculated r_{TFA} concentrations asymmetries for a case in which the transport of TFA and CF_3COX was switched off. This results in r_{TFA} asymmetries which are in much better

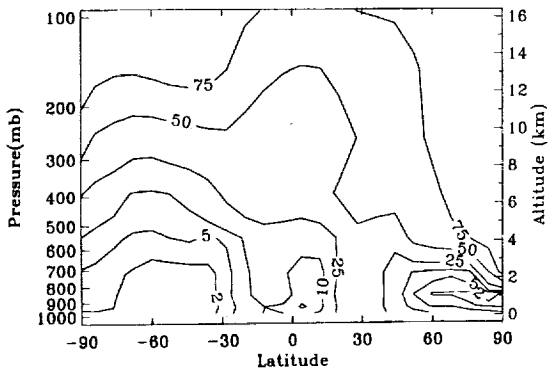

Figure 10b. CF_3COF mixing ratios (1.0E-3 pptv) averaged over a latitude band for the month of July in the year 2010.

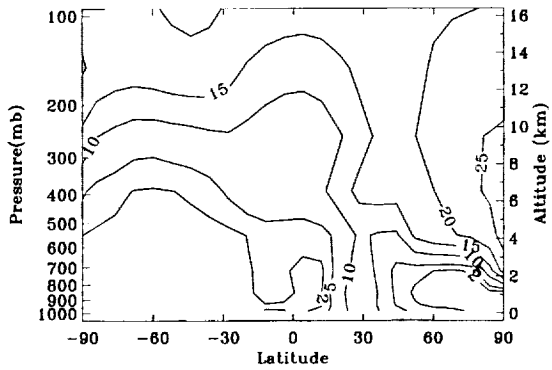

Figure 11b. CF_3COCl mixing ratio (1.0E-3 pptv) averaged over a latitude band for the month of July in the year 2010.

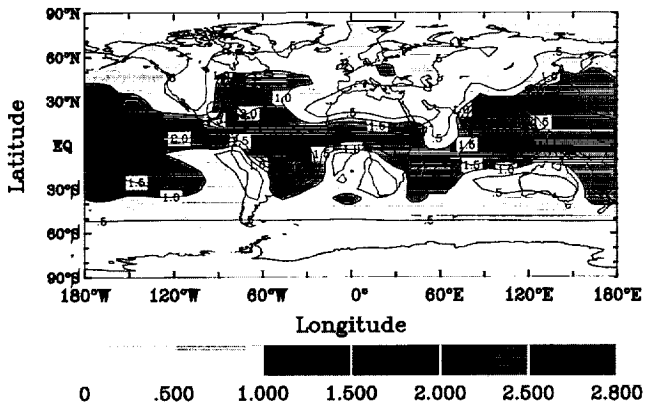

Figure 12. Cumulative amount of TFA deposited by wet processes by the year 2010 at the surface in mg/m^2.

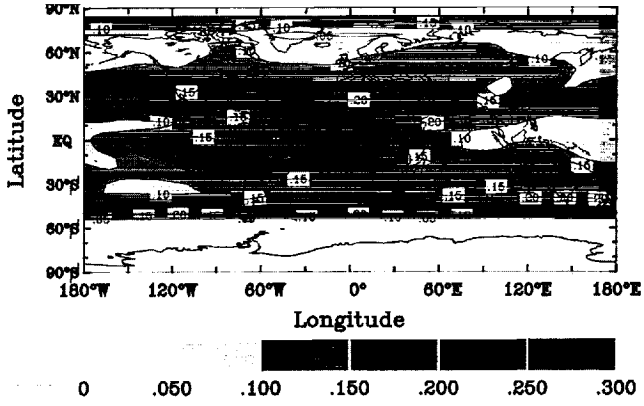

Figure 14. Annual average TFA in rainwater (μg/L) for the year 2010.

agreement with the rainfall asymmetries. Thus inclusion of transport substantially "smoothes out" the asymmetries in r_{TFA} expected from simple consideration of asymmetries in rainout and OH fields.

The competition between transport and local production removal in determining r_{TFA} has an even larger impact on the expected variability of r_{TFA} in a given geographical region. The r_{TFA} concentrations calculated for the year 2010 in all the grid boxes of the model and for all the months of the year (36 longitude $\times$ 24 latitude $\times$ 12 months) are presented in the form of a box plot in Figure 17. The data were binned by the amount of rainfall received in mm/month. The vertical axis shows the concentrations of r_{TFA} in μg/L. Although the median r_{TFA} is fairly constant around 0.12 μg/L for all the bins, the range in the r_{TFA} concentrations at low levels of rainfall is larger compared to the bins with larger rainfall amounts. This reflects primarily the impact of transport when local removal time constants become small. We can thus expect the largest uncertainty in the calculation in regions, where many of the seasonal water bodies of concern are located. In these cases, resolution of synoptic variability in the transport is necessary for a better estimate.

5. Discussion of Uncertainties

Our approximations for both in-cloud hydrolysis and washout are very simplistic, assuming an average, continuous rate over the grid box, where in actuality these are sporadic events. A better approach would need to consider, for example, coupling to moist convection events and large-scale rain [*Balkanski et al.*, 1993]. Thus our calculations disregard the coupling between clouds, rainout, and transport. We have carried out limited simulations to study the sensitivity of our results to our assumption of continuous hydrolysis and washout rates versus episodic cloud and rain events as well as in-cloud residence time. By varying the cloud cover, residence time, and washout we can gain information as to the magnitude of the error introduced in this decoupling. Finally, we also consider the sensitivity to the large uncertainty in the removal rates at high latitudes as well as to the adopted concentrations of OH.

5.1. Sensitivity of TFA Production to Intermittent Cloud Cover

Observations indicate that on a global average, a given location on land can go completely cloud free between 17% and 19% of the time. Over oceans the completely cloud free time is observed to drop to 3% of the total time [*Warren et al.*, 1986, 1988]. We performed numerical experiments, with cloud cover switched on for 24 hours every 4 days (75% cloud free) and every 7 days (85% cloud free). Loss frequencies for $CF_3C(O)X$ were, however, adjusted to yield the same average frequency over the whole period of time. All the simulations discussed below were performed for CF_3COF produced from HFC-134a alone and for the year 2010 only.

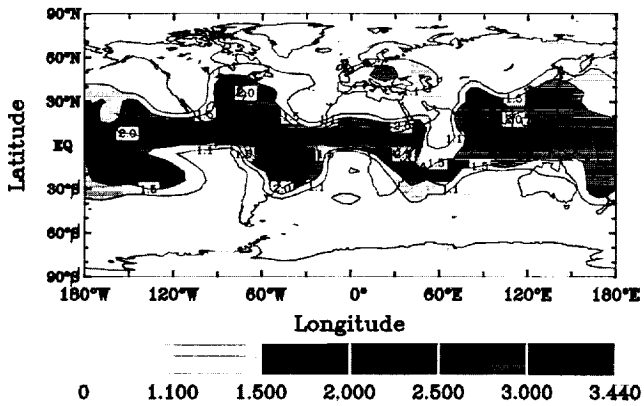

Figure 13. Cumulative amount of TFA deposited by wet and dry processes by the year 2010 at the surface in mg/m^2.

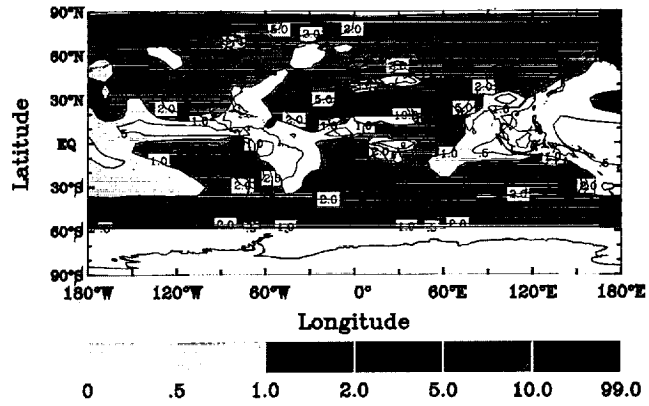

Figure 15. Annual average asymmetries in rainfall amounts. Figure show ratios of global average/grid average amounts.

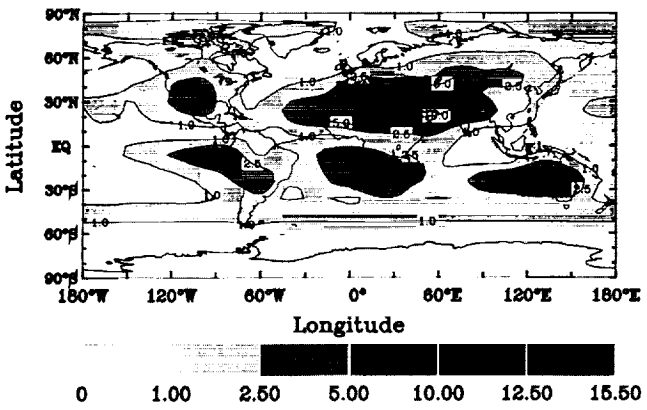

Figure 16. Annual average r_{TFA} asymmetries for the year 2010 from global average concentrations for the "no transport" case.

In the subtropical regions, TFA production increases by an average of 30% with local increases of up to 50%. TFA production at middle and high latitudes changed by only a few percent. Thus the effect of intermittent cloud cover on annual average TFA production from the hydrolysis of CF_3COF can be expected to result in a maximum of 30% increase on a regional scale.

5.2. Sensitivity of TFA Washout to Intermittent Rain

The effect of intermittent rainfall on washout rates was investigated in detail by *Giorgi and Chameides* [1985], *Thompson and Cicerone* [1982], and *Stewart et al.* [1983] employing one-dimensional models. In general, it was noted that the increase in frequency of the rainfall shortens the washout lifetime of the species, and for the case of a highly soluble species, the washout rate is proportional to the rainfall frequency. Here rainfall frequency refers to the number of rainfall events occurring in a given time. The higher the frequency, the larger the number of rainfall events that occur, eventually leading to the continuous rainfall and continuous washout.

We studied the ratio of r_{TFA} obtained for the continuous rainfall case to a case where rain occurs once every 7 days for one full day. This is an extreme case. The washout rate and rain amount for the intermittent rainfall cases were adjusted such that the total rate for a particular month remains the same for all the cases. In locations (Indian Ocean and eastern Pacific regions) with the highest calculated r_{TFA}, the new r_{TFA} goes up by as much as 30%. Increases of up to 20% are obtained in the western United States and up to 25% in the southwestern United States and southern Africa and China.

5.3. Sensitivity of r_{TFA} to in-Cloud Residence Time

We also examined the sensitivity of our calculations by increasing the in-cloud residence time (with a value of 1.2 hours) to 3 hours and decreasing it to 0.8 hours. The residence times will have 10–20% effect on r_{TFA} concentrations in locations receiving low rainfall (subtropical Asia, Africa, southwestern United States, and the northwestern location of South America). The effect on regions receiving high amounts of rainfall is less than 15%, and changes of the order of 1–5% were obtained over the rest of the domain.

5.4. Sensitivity of r_{TFA} to Washout South of 60°S

The washout rates from 45°S to 90°S were calculated on the basis of the climatology of *Jaeger* [1976]. However, values south of 60°S are very uncertain, in particular since it is difficult to distinguish between rain and snow. The influence of increased washout (rainfall) in this zonal region on r_{TFA} concentrations were examined by increasing the washout rate beyond 60°S by a factor of 2. Increasing rainfall in the southern latitudes will decrease r_{TFA} by 10% in some locations to the south of 60°S but has no significant effect over the rest of the model domain.

5.5. Sensitivity of r_{TFA} to OH Concentration

We also examined the sensitivity of our calculations to a 20% increase in the OH fields used for calculating the degradation of the TFA precursor HFC-134a. Results indicate that the lifetime of HFC-134a decreases by 16%, and the global average HFC-134a mixing ratios is reduced by 6% from the base case discussed in section 4. The global average r_{TFA} increases by 12%. Because of an increase in dry deposition over arid subtropical regions of Africa and Asia compared to the base case, local increases of the order of 2–10% are obtained in these regions.

5.6. Impact of Reduction in the TFA Yield From HFC-134a

As discussed above, recent experimental results reported by *Wallington et al.* [1996] suggest that the reaction of CF_3CFHO_2 with NO yields primarily vibrationally excited CF_3CHFO radicals. These radicals will undergo prompt thermal fission, unless they are thermalized by collisions with ambient molecules. The experiments suggest that about 40% of the excited CF_3CFHO_2 is thermalized. Since reaction with NO is expected to be primarily the channel for degradation of CF_3CFHO_2, these results suggest that the mass yield of $CF_3C(O)F$ from HFC-134a is reduced from 37 to 15%.

The impact of these reductions on the total amount of TFA deposited will depend on the specific scenario adopted for the relative emissions of HCFC-123 and 124 and HFC-134a. For the scenario adopted in these calculations we estimate that the

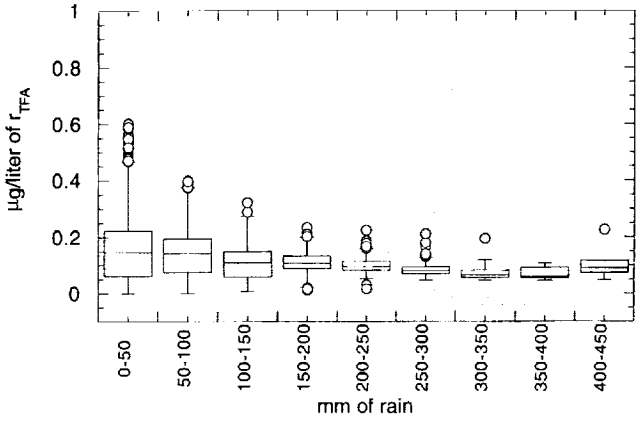

Figure 17. Boxplot of r_{TFA} versus rainfall amounts for the year 2010. Data selected for the plot are from the last year of the simulation and all the grid boxes. There is one data point per month per grid box. The bar in the middle of the box is the median of the data and the boxes represent the middle 50% of the data binned in the grid. The whiskers represent the acceptable range of the remaining data beyond that located inside the box. Outliers are denoted by points.

calculated-global-averaged TFA concentrations in rainwater will decrease by 26%, i.e., from 0.12 to 0.09 μg/L.

6. Conclusions

We have carried out simulations of the degradation of HFC-134a and HCFC-123 and HCFC-124, with emphasis on the production of TFA and its concentration in rainwater. The complicated degradation schemes for these precursors have been considerably simplified, taking advantage of the fact of the short chemical time constants of most intermediate species. We tested the sensitivity of the calculated rainwater concentration of TFA (r_{TFA}) to various parameterizations and approximations adopted in the model. Our limited sensitivity studies suggest that these approximations would not have a greater than 30% effect on the calculated r_{TFA}.

Annual average r_{TFA} concentrations in the range of 0.15–0.2 μg/L were obtained for the year 2010 in the northern midlatitudes. The calculated r_{TFA} concentrations in July 2010 in parts of North America and southern Europe were found to be 0.3–0.45 μg/L. Inclusion of a reduced yield for TFA formation from HFC-134a, suggested by *Wallington et al.* [1996], will reduce these numbers 26%. Dry deposition fluxes are on average about 20% of the wet deposition and about equal for and regions. In the absence of soil sinks, dry deposition could also contribute to accumulations in groundwater and seasonal water bodies. Assessment of this contribution would require a detailed hydrological model for the catch basins of interest.

Our simulations show the crucial role played by long-range zonal transport of gas phase TFA and $CF_3C(O)X$ in smoothing out the chemical impact of asymmetries in the OH and rainfall fields. Transport effects become important when advective time constants become comparable to those of other transformation and deposition processes, a condition that is true most everywhere for gas phase TFA. Thus in spite of the short time constants for hydrolysis and washout, simulation of the TFA distribution does require use of three-dimensional models. Transport processes are particularly important in regions, where removal rates are slower. Our results show that these regions exhibit the largest variance in the calculated r_{TFA}.

The results presented here can be tested as measurements of TFA, and its precursors become available. The calculated mixing ratios of HCFC-124 and HCFC-123 for NH are 1.96 and 0.21, and global averages are 1.56 and 0.14 pptv, respectively, for July 1995. For the 1995 conditions the contributions of the three precursors to the total r_{TFA} in western Europe (0.014 μg/L) break down as follows: 57% from HCFC-124, 27% from HCFC-123, and 16% from HFC-134a. Thus in the short term the greatest impact on r_{TFA} could be from shorter-lived HCFC-124 and HCFC-123, and it is advisable to monitor their emissions.

Measurements of HFC-134a, starting from the year 1990 to 1995, were reported by *Montzka et al.* [1996] and *Oram et al.* [1996]. *Montzka et al.* [1996] report a mixing ratio of 2.33 pptv in the NH, 1.13 in the SH, and a global average mixing ratio of 1.73 pptv for the beginning of July 1995. The model-calculated mixing ratios for this period are 3.4 pptv for the NH, 1.48 pptv for the SH, and a global average of 2.44 pptv. This discrepancy is a reflection of the fact that this study used projected rather than actual emissions for this compound for the period of interest.

Measurements of TFA in natural water bodies and rainwater in the western United States were reported by *Zehavi and Sieber* [1996]. It is difficult to compare their measurements for natural waters, since we have not carried out a detailed study of the local chemistry, transport, and hydrology. Measured rainwater concentrations range from 0.03 to 0.09 μg/L, a factor of 2–6 larger than our calculated values for the western United States in 1995 (0.015 μg/L). Measurements of r_{TFA} have been made at two locations in western Europe [*Frank et al.*, 1996]. The measured r_{TFA} is in the range of 0.025–0.28 μg/L for the year 1995 at Bayreuth, Germany, and in the range of 0.04–0.08 μg/L at Zurich and Alpthal, Switzerland. The mean r_{TFA} for all the measurements is 0.1 μg/L. The measured gas phase concentrations of TFA are of the order of 0.01 pptv. The gas phase TFA mixing ratios calculated in the present study are in the range of 0.007–0.005 pptv for western Europe for the year 1995. The calculated annual average r_{TFA} for the year 1995 is 0.014 μg/L in western Europe. These numbers would have to be rescaled when measurements of the precursors are available. In the case of HC 134a, this would imply a contribution of 0.0015 μg/Liter, based on the measurements of *Montzka et al.* [1995]. Although no measurements for HCFC 123 and HFC 124 are available, it is doubtful that the actual concentrations are higher than the calculated concentrations.

The higher r_{TFA} concentrations measured could be due to additional unknown sources as suggested by *Frank et al.* [1996]. We note, however, that given the limited number of samples collected and the large variability of the measurements, the reported concentrations cannot be considered a true mean for the region (i.e., our coarse grid box). Great caution should be exercised in comparing the calculated grid average concentrations and global average concentrations of r_{TFA} to a small number of local measurements. Given the sensitivity of the calculated present-day r_{TFA} to the amount HCFC-124 and HCFC-123 emitted, it would be of great value to measure these compounds in the atmosphere. A monitoring program for the concentrations of TFA and its precursors could help ascertain the actual variability of the rainwater concentrations.

Acknowledgments. This work was funded by the Alternative Fluorocarbon Environmental Acceptability Study (AFEAS) and by NASA's Atmospheric Chemistry Modeling and Analysis Program (ACMAP). We also wish to acknowledge the support of ARC (Atmospheric Research Council) of CMA (Chemical Manufacturers Association) for funding the initial phases of 3-D model acquisition and implementation.

References

Atkinson, R., Tropospheric reactions of the haloalkyl radicals formed from hydroxyl radical reaction with a series of alternative fluorocarbons, in *WMO Scientific Assessment of Stratospheric Ozone*, vol. II, pp. 165–208, World Meteorol. Organ., Geneva, 1989.

Balkanski, Y. J., D. J. Jacob, G. M. Gardner, W. C. Graustein, and K. K. Turkeian, Transport and residence times of tropospheric aerosols inferred from a global three-dimensional simulation of ^{210}Pb, *J. Geophys. Res.*, *98*, 20,573–20,586, 1993.

Carr, S., J. J. Treacy, H. W. Sidebottom, R. K. Connell, C. E. Conosamas, R. P. Wayne, and J. Franklin, Kinetics and mechanisms for the reaction of hydroxyl radicals with trifluoroacetic acid under atmospheric conditions, *Chem. Phys. Lett.*, *227*, 39–41, 1994.

DeMore, W. B., D. M. Golden, R. F. Hampson, M. J. Kurylo, C. J. Howard, A. R. Ravishankara, C. E. Kolb, and M. J. Chemical *Chemical kinetics and photochemical data for use in stratospheric modeling, in Evaluation 10, JPL Publ. 92–20*, NASA/Jet Propul. Lab., Pasadena, Calif., 1992.

Exner, M., H. Herrmann, J. Michel, and R. Zellner, Hydrolysis rate of CF_3COF and the decarboxylation of CF_3COO^- anions, in *AFEAS Workshop Proceedings: Atmospheric Wet and Dry Deposition of Car-*

bonyl and Haloacetyl Halides, Solvay Res. and Technol. Cent., Brussels, 1992.

Frank, H., A. Klein, and D. Renschen, Environmental trifluoroacetate, *Nature*, *382*, 34, 1996.

Franklin, J., The ATmospheric degradation and impact of 1,1,1,2-Tetrafluoroethane (Hydrolfluorocarbon 134a), *Chemosphere*, *27*, 1565–1601, 1993.

Freiberg, J. E., and S. E. Schwartz, Oxidation of SO_2 in aqueous droplets: Mass-transport limitations in laboratory studies and ambient atmosphere, *Atmos. Environ.*, *15*, 1145–1154, 1980.

George, C., J. L. Ponche, P. Mirabel, Experimental determination of uptake coefficient for acid halides, paper presented at the STEP-HALOCSIDE/AFEAS Workshop, 23–25 Altern. Fluorocarbons Environ. Acceptability Study (AFEAS), March, Dublin, 1993.

Giorgi, F., and W. L. Chameides, The rainout parameterization in a photochemical model, *J. Geophys. Res.*, *90*, 7872–7880, 1985.

Hansen, J., G. Russell, D. Rind, P. Stone, A. Lacis, S. Lebedeff, R. Ruedy, and L. Travis, Efficient three-dimensional global models for climate studies: Models I and II, *Mon. Weather Rev.*, *111*, 609–662, 1983.

Intergovernmental Panel on Climate change (IPCC), Climate change—The IPCC scientific assessment, World Meteorol. Organ./ United Nations Environ. Programme (WMO/UNEP), Geneva, 1990.

IPCC, Climate change 1995—Impacts, adaptations and mitigation of climate change: *Scintific* technical analyses, WMO/UNEP, Geneva, 1996.

Jacob, D. J., and M. J. Prather, Radon-222 as a test of convective transport in a general circulation model, *Tellus Ser. B.*, *42*, 118–134, 1990.

Jacob, D. J., M. Prather, S. Wofsy, and M. McElroy, Atmospheric distribution of ^{85}Kr simulated with a general circulation model, *J. Geophys. Res.*, *92*, 6614–6626, 1987.

Jaeger, L.,*Selbstverlag des Deutschen Wetterdienstes, Ber. Dtsch. Wetterdienstes n.139(18)*, Offenbach am Main, Germany, 1976.

Jaeger, L. Monthly and areal patterns of mean global precipitation, edited by A. Street-Perrott et al., in *Variations in the Global Budget*, 129 pp., D. Reidel, Norwell, Mass., 1983.

Kanakidou, M., F. J. Dentener, and P. J. Crutzen, A global three-dimensional study of the fate of HCFCs and HFC-131a in the troposphere, *J. Geophys. Res.*, *100*, 18,781–18,801, 1995.

Kotamarthi, V. R., and G. R. Carmichael, The long range transport of pollutants in the Pacific region, Atmos.. Environ., 1521–1534, 1990.

Lelieveld, J., and P. J. Crutzen, Influences of cloud photochemical processes on tropospheric ozone, *Nature*, *343*, 227–233, 1990.

Lelieveld, J., P. J. Crutzen, and H. Rodhe, *Zonal Average Cloud Characteristics for Global Atmospheric Chemistry Modeling*, 51 pp., Int. Meteorol. Inst. Stockholm, 1989.

Logan, J. A., M. J. Prather, S. C. Wofsy, and M. B. McElroy, Tropospheric chemistry: A global perspective, *J. Geophys. Res.*, *86*, 7210–7254, 1981.

McCulloch, A., P. M. Midgley,, and D. A. Fisher, Distribution of emissions of chlorofluorocarbons (CFCs) 11, 12, 113, 114 and 115 among reporting and non-reporting countries in 1986, *Atmos. Environ.*, *28*(16), 2567–2582, 1994.

Montzka, S. A., R. C. Myers, J. H. Butler, J. W. Elkins, L. T. Lock, A. D. Clarke, and A. H. Goldstein, Observations of HFC-134a in the remote troposphere, *Geophys. Res. Lett.*, *23*, 169–172, 1996.

NASA, Report on concentrations lifetimes, and trends of CFCs, halons, and related species, *NASA Ref. Publ. 1339*, 1994.

Oram, D. E., C. E. Reeves, W. T. Sturges, S. A. Penkett, P. J. Frases, and R. L. Langenfelds, Recent tropospheric growth rate and distribution of HFC-134a (CF_3CH_2F), *Geophys. Res. Lett.*, *23*, 1949–1952, 1996.

Prabhakara, C., I. Wang, A. T. C. Chang, and P. Gloersen, A statistical examination of Nimbus-7 SMMR data and remote sensing of sea surface temperature, liquid water content in the atmosphere and surface wind speed, *J. Appl. Meterol.*, *22*, 2023–2037, 1983.

Prather, M. J., and C. M. Spivakovsky, Tropospheric lifetimes of hydrochlorofluorocarbons, *J. Geophys. Res.*, *95*, 18,723–18,729, 1990.

Prather, M. J., M. McElroy, S. Wofsy, G. Russell, and D. Rind, Chemistry of global troposphere: Fluorocarbons as tracers of air motion, *J. Geophys. Res.*, *92*, 6579–6613, 1987.

Prinn, R. G., R. F. Weiss, B. R. Miller, J. Huang, F. N. Alayea, D. M. Cunnold, P. J. Fraser, D. E. Hartley, and P. G. Simmonds, Atmospheric trends and lifetime of CH_3CCl_3 and global OH concentrations, *Science*, *269*, 187–192, 1995.

Rattigan, O., R. A. Cox, and R. L. Jones, The UV absorption cross-section of CF_3COCl, CF_3COF, CH_3COF and CCl_3CHO, paper presented by the STEP-HALOCSIDE/AFEAS Workshop, Afeas, May 14–16, Dublin, 1991.

Rodriguez, J. M., M. K. W. Ko, N. D. Sze, and C. W. Heisey, Two-dimensional assessment of the degradation of HFC-134a: Tropospheric accumulations and deposition of trifluoroaacetic acid, in *Kinetics and Mechanisms for the Reactions of Halogenated Organic Compounds in the Troposphere*, AFEAS, Univ. College, Dublin, 1993.

Schwartz, S. E., Mass-transport considerations pertinent to aqueous phase reactions of gases in liquid-water clouds, in *Chemistry of Multiphase Atmospheric Systems*, edited by W. Jaeschke, vol. G6, Springer-Verlag, New York, 1986.

Shea, D. J., Climatological atlas: 1950-1979, *NCAR Tech. Note, NCAR/TN-269+STR*, NAH. Cent. for Atmos. Res., Boulder, Colo., 1986.

Spivakovsky, C. R., R. Yevich, J. Logan, S. Wofsy, M. McElroy, and M. Prather, Tropospheric OH in the three-dimensional chemical tracer model: An assessment based on observations of CH_3CCl_3, *J. Geophys. Res.*, *95*, 18,433–18,439, 1990.

Stewart, R. W., S. Hameed, and G. Matloff, A model study of the effects of intermittent loss on odd nitrogen concentrations in the lower troposphere, *J. Geophys. Res.*, *88*, 10,697–10,707, 1983.

Thompson, A. M., and R. J. Cicerone, Clouds and wet removal as causes of variability in the trace-gas composition of the marine troposphere, *J. Geophys. Res.*, *87*, 8811–8826, 1982.

Tromp, T. K., M. K. W. Ko, J. M. Rodriquez, and N. D. Sze, Potential accumulations of a CFC-replacement degradation product in seasonal wetlands, *Nature*, *376*, 327–330, 1995.

Tuazon, E. C., and R. Atkinson, Tropospheric degradation products of CH_2FCF_3, (HFC-134a), *J. Atmos. Chem.*, *16*, 301–312, 1993.

Visscher, P. T., C. W. Culbertson, and R. S. Ormeland, Degradation of trifluoroacetate in oxic and anoxic environments, *Nature*, *369*, 729–731, 1994.

Wallace, J. M., and P. V. Hobbs, *Atmospheric Science: An Introductory Survey*, vii-467, Academic, San Diego, Calif., 1977.

Wallington, T. J., M. D. Hurley, J. C. Ball, and E. W. Kaiser, Atmospheric Chemistry of Hydrofluorocarbon 134a, Fate of alkoxy radical CF_3CFHO, *Environ. Sci. Technol.*, *26*, 1318–1324, 1992.

Wallington, T. J., M. D. Hurley, J. M. Fracheboud, J. J. Orlando, G. S. Tyndall, J. Sehsested, T. E. Mogelberg, and O. J. Nielsen, Role of excited CF_3CFHO radicals in the atmospheric chemistry of HFC-134a, *J. Phys. Chem.*, *100*, 18,116–18,122, 1996.

Warren, S. G., C. J. Hahn, J. London, R. M. Chervin, and R. L. Jenne, Global distribution of total cloud cover an cloud type amounts over land, *NCAR Tech. Note, NCAR/TN-273+STR, Natl. Cent. for Atmos. Res., Boulder, Colo., 1986.*

Warren, S. G., C. J. Hahn, J. London, R. M. Chervin, and R. L. Jenne, Global distribution of total cloud cover and cloud type amounts over the ocean, *NCAR Tech. Note, NCAR/TN-317+STR, Natl. Cent. for Atmos. Res., Boulder, Colo., 1988.*

Wine, P. H., and W. L. Chameides, Possible atmospheric lifetimes and chemical reaction mechanisms for selected HCFCs, HFCs, CH_3CCl_3, and their degradation products against dissolution and/or degradation in seawater and cloudwater, in Scientific Assessment of Stratospheric Ozone: 1989, AFEAS, Rep. *20*, World Meteorol. Oragan., Global Ozone Res. and Monit. Proj., Geneva, 1990.

World Meteorological Organization (WMO), Scientific Assessment of Stratospheric Ozone: 1989, *WMO Rep.*, *20*, Global Ozone Res. and Monit. Proj. U.N. Environ. Program, World Meteorol. Organ., Geneva, 1990.

Zehavi, D., and Seiber, J. N., An analytical method for trifluoroacetic acid in water and air samples using headspace gas chromatographic determination of the methyl ester, *Anal. Chem.*, *68*, 3450–3459, 1996.

M. K. W. Ko, V. R. Kotamarthi, J. M. Rodriquez, N. D. Sze, and T. K. Tromp, Atmospheric and Environmental Research, Inc., 840 Memorial Drive, Cambridge, MA 02139-3794. (e-mail: jose@aer.com)

M. J. Prather, Earth System Science, University of California, Irvine, CA 92717.

(Received November 22, 1996; revised October 1, 1997; accepted October 13, 1997.)